The Journal of the Acoustical Society of America

OCTOBER 08 2024

Detection of mild sensory hearing loss using a joint reflection-distortion otoacoustic emission profile

Carolina Abdala; Tricia Benjamin; Samantha Stiepan; Ping Luo; Christopher A. Shera

Check for updates

J. Acoust. Soc. Am. 156, 2220–2236 (2024)
https://doi.org/10.1121/10.0030399

View Online
Export Citation

Articles You May Be Interested In

Towards a joint reflection-distortion otoacoustic emission profile: Results in normal and impaired ears

J. Acoust. Soc. Am. (August 2017)

Relationships between preference ratings, sensory profiles, and acoustical measurements in concert halls

J. Acoust. Soc. Am. (January 2014)

Blast exposure in the military and its effects on sensory and cognitive auditory processing

J Acoust Soc Am (March 2019)

31 October 2024 19:47:36

Take the Lead in Acoustics

The ability to account for coupled physics phenomena lets you predict, optimize, and virtually test a design under real-world conditions – even before a first prototype is built.

» Learn more about COMSOL Multiphysics®

COMSOL

ASA ACOUSTICAL SOCIETY OF AMERICA

JASA ARTICLE

Detection of mild sensory hearing loss using a joint reflection-distortion otoacoustic emission profile

Carolina Abdala,[a] Tricia Benjamin, Samantha Stiepan, Ping Luo, and Christopher A. Shera
Caruso Department of Otolaryngology, Keck School of Medicine, University of Southern California, 1640 Marengo Avenue, Suite 326, Los Angeles, California 90033, USA

ABSTRACT:
Measuring and analyzing both nonlinear-distortion and linear-reflection otoacoustic emissions (OAEs) combined creates what we have termed a "joint-OAE profile." Here, we test whether these two classes of emissions have different sensitivities to hearing loss and whether our joint-OAE profile can detect mild-moderate hearing loss better than conventional OAE protocols have. $2f_1$-f_2 distortion-product OAEs and stimulus-frequency OAEs were evoked with rapidly sweeping tones in 300 normal and impaired ears. Metrics included OAE amplitude for fixed-level stimuli as well as slope and compression features derived from OAE input/output functions. Results show that mild-moderate hearing loss impacts distortion and reflection emissions differently. Clinical decision theory was applied using OAE metrics to classify all ears as either normal-hearing or hearing-impaired. Our best OAE classifiers achieved 90% or better hit rates (with false positive rates of 5%–10%) for mild hearing loss, across a nearly five-octave range. In summary, results suggest that distortion and reflection emissions have distinct sensitivities to hearing loss, which supports the use of a joint-OAE approach for diagnosis. Results also indicate that analyzing both reflection and distortion OAEs together to detect mild hearing loss produces outstanding accuracy across the frequency range, exceeding that achieved by conventional OAE protocols. © *2024 Acoustical Society of America.*
https://doi.org/10.1121/10.0030399
(Received 28 May 2024; revised 9 August 2024; accepted 11 September 2024; published online 8 October 2024)
[Editor: Hideko Heidi Nakajima] Pages: 2220–2236

31 October 2024 19:47:36

I. INTRODUCTION

In the decades following the discovery of otoacoustic emissions (OAEs) (Kemp, 1978), research studies sought to define their basic features [e.g., Brown and Kemp (1984), Kemp *et al.* (1986), Probst *et al.* (1987), Martin *et al.* (1990), Lonsbury-Martin *et al.* (1990), and Smurzynski and Kim (1992)] and probe their clinical utility [e.g., Gorga *et al.* (1993a), Gorga *et al.* (1993b), Prieve *et al.* (1993), Kim *et al.* (1996), Stover *et al.* (1996), Gorga *et al.* (1997), Hussain *et al.* (1998), Dorn *et al.* (1999), Ellison and Keefe (2005), Johnson *et al.* (2007), and Go *et al.* (2019)]. This effort produced a significant body of literature estimating the accuracy with which distortion-product and transient-evoked OAEs could classify ears as normal or hearing-impaired. This body of work, much of it from the prolific group at Boys Town National Research Hospital, showed that distortion-product otoacoustic emissions (DPOAEs) measured in large groups of subjects with hearing loss ranging from mild to profound, detected sensory hearing loss around 4 kHz with acceptable accuracy (~80%–85%); at lower and higher frequencies, however, performance was much worse [e.g., Gorga *et al.* (1997)]. Transient-evoked OAEs, in contrast to DPOAEs, detected hearing loss best at frequencies around 1–2 kHz, also in groups of subjects with mild-to-profound degrees of hearing loss (Gorga *et al.*, 1993b; Prieve *et al.*, 1993). The detection of hearing loss with OAEs improved when a multivariate approach was implemented, which typically involved the inclusion of predictive information across several frequencies combined (Hussain *et al.*, 1998; Dorn *et al.*, 1999; Gorga *et al.*, 2005). Multivariate strategies achieved roughly 90% hit rates or better (with acceptable false-alarm rates) at frequencies around 3–4 kHz but hit rates approximating 70%–85% at lower frequencies (Gorga *et al.*, 2005). These early studies yielded recommendations for the optimal stimulus parameters to achieve diagnostic accuracy [e.g., Stover *et al.* (1996)]. In fact, current default protocols commonly applied in OAE clinical assessment today are derived from this work, with little deviation over two decades.

A. Theoretical and practical advances

In 1999, Shera and Guinan (1999) described a novel model of OAE generation. The dual-source model held that *nonlinear-distortion* emissions, such as the $2f_1$-f_2 DPOAE, arise via the saturation of outer-hair-cell transduction currents [e.g., Hudspeth and Corey (1977)] and they probe the strength and form of cochlear nonlinearities. *Linear-reflection* emissions, such as transient-evoked or stimulus-evoked OAEs, are thought to be backscattered wavelets, reflected off randomly situated micromechanical irregularities along the cochlear partition (Zweig and Shera, 1995; Shera and Guinan, 1999). At low sound levels, the reflected wavelets

[a]Email: Carolina.Abdala@usc.edu

 © 2024 Acoustical Society of America

https://doi.org/10.1121/10.0030399

come primarily from the region near the peak of the traveling wave (Lichtenhan, 2012; Berezina-Greene and Guinan, 2015; Goodman *et al.*, 2020) and probe features characteristic of this region such as near-threshold tuning and low-level amplifier gain. While the two emission sources arise via distinct generation processes, they share a common dependence on outer hair cell-based amplification. Much experimental evidence supports the dual-source model of OAE generation [e.g., Konrad-Martin *et al.* (2002), Mauermann and Kollmeier (2004), Abdala and Dhar (2010, 2012), and Abdala *et al.* (2018a)], which continues to prompt intriguing research questions: *Do each of the two classes of emissions offer non-redundant information about cochlear function and dysfunction?* If so: *Could their combined measurement/analysis improve the accuracy with which OAEs detect hearing loss?*

Recent methodological advances for evoking, analyzing, and calibrating OAEs have increased their efficiency and precision and made it possible to explore these intriguing questions. One such innovation is the use of rapid, continuously *sweeping* tones as stimuli (Choi *et al.*, 2008; Long *et al.*, 2008; Bennett and Özdamar, 2010; Kalluri and Shera, 2013; Abdala *et al.*, 2015; Shera, 2024) vs conventional methods presenting discrete tones at fixed frequencies. OAEs evoked by sweeping tones provide unparalleled frequency resolution and up to 10 times the time efficiency compared to discrete tones (Abdala *et al.*, 2015). Importantly, it has also been shown that swept-tone OAEs produce matching amplitude and phase to that of conventionally measured emissions (Long *et al.*, 2008; Kalluri and Shera, 2013; Abdala *et al.*, 2015; Glavin *et al.*, 2023). The added speed of swept tones has made it possible to record both classes of OAEs—reflection and distortion—together in the same ear (Abdala *et al.*, 2022), rather than arbitrarily choosing one or the other emission. Exploiting the efficiency of sweeping tones has allowed us to access both intracochlear generation processes with what we term a "joint (reflection-distortion) OAE profile."[1]

Another recent advance in OAE methodology has been the specification of the stimulus in forward pressure level (dB FPL). This form of stimulus calibration is applied to correct for the effects of ear-canal standing waves by controlling the amplitude of the *forward* stimulus wave, separating it from any energy reflected off the tympanic membrane [Scheperle *et al.* (2008), Scheperle *et al.* (2011), and Souza *et al.* (2014)]. The interference between reflected and forward waves in the ear canal leads to inaccurate control of stimulus level at the eardrum and likely contributes to the large variability in OAE amplitude observed across individuals and upon repeated testing (Reuven *et al.*, 2013; Souza *et al.*, 2014; Maxim *et al.*, 2019). The OAE emerging from the cochlea is similarly impacted by standing waves in the enclosed ear canal; its level can be corrected using emitted pressure level (EPL) or dB EPL (Charaziak and Shera, 2017).

Progress in our understanding of OAE generation, combined with numerous advances in methodology, call for a renewed look at how hearing loss affects OAEs and a re-examination of their clinical utility. There are two aims in this study: (1) To test whether the two classes of emissions (reflection, accessed as stimulus-frequency otoacoustic emissions or SFOAEs, and distortion, accessed as the nonlinear component of the $2f_1$-f_2 DPOAE) have different sensitivities to cochlear pathology; and (2) to examine whether the joint-OAE profile improves the detection of mild sensory hearing loss relative to past work.

II. METHODS

A. Subjects

OAE data from 300 human ears were collected: One ear from 117 normal-hearing individuals (50 M, 67 F; mean age = 27 years, age range = 16 to 52 years) and 183 ears from 154 adults with slight-to-moderate sensorineural hearing loss of varying etiology were tested (84 M, 95 F, 4 non-binary; mean age = 55 years, age range = 14–78 years). Normal hearing was defined as audiometric thresholds $\leq$ 15 dB HL at octave and inter-octave frequencies from 0.5 to 8 kHz. Hearing-impaired subjects had at least two frequencies with audiometric thresholds between 20 and 55 dB HL; only the OAEs at frequencies with audiometric hearing loss (i.e., 20–55 dB HL) were included in this study. To exclude conductive hearing loss, individuals with air-bone gaps $>$ 10 dB or abnormal tympanograms were not accepted as subjects.

The mean audiometric thresholds for the 183 ears in the hearing-impaired (HI) group were 29, 29, 31, 32, 35, 36, 36, 39, 39 dB HL for 0.75 1, 1.5, 2, 3, 4, 6, and 8 kHz, respectively. The threshold at 0.75 was interpolated between audiometric thresholds at 0.5 and 1 kHz. The HI group was skewed heavily toward individuals with slight-to-mild hearing loss as 78% of thresholds in this group were between 20 and 40 dB HL. The individual audiometric thresholds are displayed in Fig. 3 in Sec. III, which plots SFOAE and DPOAE levels as a function of audiometric threshold for all ears.

B. Instrumentation and signal processing

A Babyface Pro USB High-Speed Audio Interface (RME Audio, Germany) and an ER-10X probe system (Etymōtic Research, Elk Grove Village, IL) controlled by custom software written in MATLAB (Mathworks, Natick, MA) were used to generate stimulus waveforms and record ear-canal pressures. Microphone voltages were amplified (+20 dB) and high-pass-filtered (300-Hz cutoff frequency) before A/D conversion. Testing was conducted with the subject reclined in an ergonomic chair within a sound-isolated IAC audiometric booth that met ambient noise standards (ANSI S3.1–1999). The probe cable was suspended from the ceiling and the probe tip was carefully positioned into the ear canal to achieve a relatively deep and stable fit, whereupon the cable was secured using a nylon headband. Subjects rested quietly or watched a subtitled video during testing.

Before each participant's arrival, Thévenin-equivalent probe parameters were obtained in the ER-10× calibrator

31 October 2024 19:47:36

(brass tube, inner diameter 7.9 mm) at room temperature using five settings of calibrator length (78.4, 64.8, 35.8, 29.7, and 24.6 mm) with the goal of achieving total "source-calibration errors" <1 (Scheperle *et al.*, 2011). The source-calibration error is a dimensionless index calculated as the sum of the squared differences between the measured and predicted cavity pressures divided by the sum of squares of the measured cavity pressures. The typical source-calibration error in our laboratory is 0.03. With these known parameters characterizing the probe, the ear-canal acoustic impedance and corresponding characteristic impedance were derived in each test ear using a wideband acoustic chirp. All stimulus levels in this experiment were measured in dB FPL. OAE levels were corrected to dB EPL.

C. OAE stimulus parameters

Stimulus tones were swept upward (for DPOAEs) or downward (for SFOAEs) across a nearly 5-octave range (0.6–16 kHz) at a rate of one octave/s. Sweep rate and direction were established from past work in our labs [Kalluri and Shera (2013), Abdala *et al.* (2015), and Shera and Abdala (2016)]. For normal hearers, the SFOAE probe was presented between 20 and 65 dB FPL, and the DPOAE L_2 was presented between 25 and 75 dB FPL, both with 5-dB step resolution. For subjects with hearing loss, the range of stimulus levels presented was based on the degree of hearing loss. For efficiency, the stimulus was never presented at levels lower than the best of the elevated audiometric thresholds (converted from dB HL to dB SPL). OAE and stimulus-level conditions were presented in random order, except for the first two conditions, which were 65 dB FPL for DPOAEs and 40 dB FPL for SFOAEs. When the degree of hearing loss was greater than 40 dB, random presentation of conditions was applied for the SFOAE.

During testing, the probe fit was monitored by noting deviations between target and measured ear-canal stimulus levels and by documenting changes in the frequency of the half-wave resonance in the ear canal. Testers initiated a probe refitting and recalibration for observed changes of >3 dB in the stimulus level or shifts in the half-wave resonance frequency of >400 Hz. Re-calibration also occurred automatically between stimulus-level conditions (or every 6 min, whichever was shorter). During any probe fit, an alert was provided to the tester if the presence of a leak was suspected. This occurred when absorbance at low frequencies was 0.2 (−7 dB) or higher (Groon *et al.*, 2015).

To further expedite data collection, rather than present a single continuous sweep across the five-octave frequency range, partial segments of the frequency span were stacked (with a 0.1 octave overlap) and presented concurrently [see Abdala *et al.* (2018b) and Abdala *et al.* (2022)]. Three concurrent segments were presented to evoke DPOAEs for stimulus levels from 25–60 dB FPL but only two stacks could be presented for stimuli >60 dB FPL, where nonlinear (e.g., suppressive) interactions between the segments were observed in pilot testing (i.e., when the stacked-sweep data deviated from the single-sweep level/phase by more than the typical test-retest variability). For SFOAEs, at the two highest stimulus levels (60- and 65-dB FPL), two frequency segments were presented concurrently while at moderate (50- and 55-dB FPL) and low (<50 dB FPL) levels, a three- and five-stack approach was applied without any notable deviation in level or phase re: the single-sweep condition.

Cubic DPOAEs at $2f_1$-f_2 were evoked with an optimized stimulus-frequency ratio which applied the f_2/f_1 shown to produce the highest DPOAE levels on average for a given frequency and stimulus-level combination (Stiepan *et al.*, 2022). Because much of our previous work with DPOAEs has been conducted using the so-called "scissors" method [$L_1 = 0.4$, $L_2 + 39$ dB (Kummer *et al.*, 1998)], we applied this same strategy here to establish primary-tone level separation. The primary-tone level separation strategy impacts the overall shape of the DPOAE input/output function (Zelle *et al.*, 2015). We also applied phase-rotation averaging to cancel the primary tones before analysis (Whitehead *et al.*, 1996). To do so, three stimulus segments with different primary-tone starting phases (ϕ) were interleaved such that the primary tones, f_1 and f_2, cancel when the responses are averaged.

SFOAEs were measured using a modified, interleaved suppression paradigm (Shera and Guinan, 1999). Responses to four stimulus combinations were measured: p_1 = probe tone alone, p_2 = probe and suppressor tone (+polarity), p_3 = probe tone alone, and p_4 = probe and suppressor tone (–polarity). The SFOAE time waveform was extracted from the four response waveforms using the formula: $p_{\mathrm{SFOAE}} = (p_1 + p_3 - p_2 - p_4)/2$. The suppressor tone (frequency f_s) was presented at 50 dB FPL for probe tones between 20 and 35 dB FPL and at +15 dB (re: probe level) for $L_p > 40$–65 dB FPL. The suppressor frequency was chosen so that $f_s/f_p = 0.95$ (Kalluri and Shera, 2007, 2013).

D. SNR-guided data collection

A custom-designed data-collection program guided by the SNR of the OAE calculated in real-time was utilized. The five-octave frequency range was divided into half-octave frequency bands denoted by the following center frequencies: 0.75, 1, 1.5, 2, 3, 4, 6, 8, and 12 kHz. In normal-hearing ears, the number of sweeps presented varied between 24 and 300 (depending on stimulus level and group) for DPOAEs, and between 24 and 500 for SFOAEs. These sweep numbers were derived from published literature (Gorga *et al.*, 1997; Ellison and Keefe, 2005; Abdala *et al.*, 2018b) and previous data collected in our laboratory.

OAE data collection ceased when SNR at all center frequencies (except 12 kHz) reached at least 6 dB, the maximum number of sweeps was reached, or the remaining sweeps allotted were unlikely to result in at least 6 dB SNR; this judgement was guided by the projected increase in SNR based on the square root of the remaining available sweeps. The mean duration of OAE data collection with this joint protocol was 43 min for normal-hearers (range = 26–68 min)

31 October 2024 19:47:36

https://doi.org/10.1121/10.0030399

and 62 min for HI subjects (range = 23–136 min). Note that while we measured across a broad parametric space in this study (requiring long data-collection sessions), the joint-OAE profile will need to be strategically abbreviated, retaining only the most effective classifiers, to create a feasible clinical protocol in the future.

E. Estimating OAEs: Least square fit and signal processing

OAE level and phase were derived from the recorded ear-canal signal at 500 frequencies across the five-octave frequency range (0.6 to 16 kHz) using an LSF procedure (Long *et al.*, 2008). Briefly, this method estimates OAE level and phase by segmenting the OAE time waveform into moving analysis windows that shift in 0.01 octave steps. Models for the stimuli, suppressors, and OAEs are created within these windows. The amplitude and phase within each window are estimated by minimizing the sum of the squared residuals between the model and the data to achieve the best fit. LSF analysis-window durations varied continuously as a function of frequency to keep constant the number of spectral fine structure periods (for DPOAEs) or cycles of phase rotation (for SFOAEs) [see Abdala *et al.* (2022) for details].

For DPOAEs, the LSF was also used to separate the nonlinear distortion component from the total DPOAE. Because the reflection component occurs at longer latencies, it can be removed by using a wide LSF analysis window (~1.75 fine-structure periods) (Long *et al.*, 2008; Abdala *et al.*, 2015). The SFOAE was processed with a continuous wavelet transform (CWT) to eliminate short-latency stimulus artifact and long-latency multiple internal reflections (Moleti *et al.*, 2012). The CWT is a time-frequency analysis tool that decomposes signals using wavelets that are frequency-scaled and time-shifted. Compared to other time-frequency analyses (e.g., the short-time Fourier transform) the CWT provides improved time resolution at high frequencies and improved frequency resolution at low frequencies. The corresponding noise floors were calculated at four points around the OAE frequency, either on the low-frequency side (0.90, 0.88, 0.86, 0.84 × DPOAE frequency) or the high-frequency side (1.10, 1.12, 1.14, 1.16 × SFOAE frequency) and then passed through the same signal processing as was the emission.

F. Artifact rejection

Following each individual sweep presentation, an LSF estimate of the OAE was derived and the median magnitude of the OAE was updated in the display. Any single data point (of the 500 frequencies sampled across frequency) differing from the real-time median OAE level by more than 4 standard deviations was considered an "artifact" and automatically triggered an additional sweep. During post-test analysis, the artifacts were identified in the frequency domain and linked to their corresponding point on the time waveform. A segment centered around this frequency and equal in duration to 20% of the LSF analysis window was eliminated. Overall, 16% of the total sweeps presented to the group with hearing loss, and 21% of those presented to normal hearers, contained rejected segments.

G. Data analysis

1. Band-averaged spectra

We did not analyze OAE data at single test frequencies as is convention; rather, we analyzed OAE data in frequency bands. OAE level and corresponding noise floors were binned into half-octave-wide frequency bands, each containing a maximum of 50 data points. These bands were centered at 0.75, 1, 1.5, 2, 3, 4, 6, 8, and 12 kHz. To prevent poor quality data, OAE data were removed if noise was excessive [see Abdala *et al.* (2022) for details]. OAE signal-to-noise ratios (SNRs) can be low for two reasons: the noise can be excessively high (for reasons that often have little to do with the generation of OAEs) or the signal can be low. We were only interested in measuring OAEs in the latter category because low-level emissions offer information about the integrity of the cochlea. Only 0.003% of the band-average data were eliminated based on excessive noise. While we did not use SNR criteria to eliminate OAEs, we did weight the contribution of each single data point to the half-octave mean by its SNR. The weighting function was the square of the SNR on a linear scale (i.e., $10^{SNR/10}$, where SNR is in dB). With this data retention strategy, even conditions with weak OAEs were represented in the half-octave band-averaged spectra although their contribution was de-emphasized.

Band-averaged spectra were analyzed at probe and L_2 levels of 40 and 65 dB FPL. The 40 dB condition represents OAE results at the lowest stimulus level providing sufficient numbers of observations (recall that not every impaired ear was tested at the lower stimulus levels), and the 65 dB condition represents OAE results for a moderate-high level stimulus.

2. Input/Output functions

OAE input/output (I/O) functions were generated at frequencies corresponding to fine-structure peaks/plateaus in SFOAE spectra measured at 50–60 dB FPL. A peak was defined as having at least a 2 dB peak-to-trough amplitude and SNR ≥ 6 dB. DPOAE I/O functions were generated at corresponding frequencies. This method of choosing test frequencies at SFOAE spectral peaks has been implemented by our labs for over a decade and described in multiple published reports. Only peak data are considered because SFOAE minima do not always reflect cochlear status (Shera and Bergevin, 2012; Kalluri and Shera, 2013; Abdala and Kalluri, 2017). Models indicate that sharp valleys result from destructive phase interactions among reflected wavelets; hence, large and erratic shifts in amplitude can occur at frequencies near these minima. In past work, we have shown that including data at frequencies corresponding to dips in SFOAE fine structure degrades test-retest reliability and reduces overall SNR (Abdala *et al.*, 2018b).

31 October 2024 19:47:36

OAE I/O functions were obtained using data within a quarter-octave frequency band around the spectral peak described above. Because OAE peaks shift slightly in frequency as the stimulus level decreases, only the top 30% of data points in the quarter-octave band contributed to the I/O function. This allowed us to more consistently track data at the peak frequency as stimulus levels decreased and avoid the inclusion of data points on a flank or minimum when analyzing data at the lowest stimulus levels. The noise floor was calculated from the same 30% of frequencies. The individual I/O functions were slotted into half-octave bands designated by their center frequency, 0.75, 1, 1.5, 2, 3, 4, 6, 8, 12 kHz. Therefore, an I/O function at a center frequency of 1 kHz, for example, might include data coming from any frequency between 0.84 to 1.20 kHz, and so on for each function.

To characterize and quantify OAE growth slope and compression features, I/O functions were fit with the following function converted to dB:

$$Y = A_n[1 + (X/A_0)^a / (1 + X/A_1)^{(a-b)}],$$

where X is stimulus amplitude in μPa; Y is OAE amplitude in μPa; A_0, A_1, A_n, a, b are fitting parameters; A_0, A_1, A_n are sound-pressure amplitudes in μPa; and a, b are power-law exponents. Conceptually, A_n is the noise amplitude, A_0 is the stimulus amplitude where the I/O function emerges from the noise, and A_1 characterizes the stimulus amplitude at the onset of the high-level behavior. The following parameters were estimated from each I/O function: (1) maximum slope (dB/dB) is the slope of the function at its steepest point; (2) source strength (dB) is the OAE level re: stimulus level at maximum slope; and (3) compression knee (dB FPL) is the stimulus level at which the slope of the function has decreased to 50% of the maximum slope. Figure 1 shows an example of one SFOAE and DPOAE I/O function with the fit described above (fit is red for SFOAE and blue for DPOAE). We cleaned the I/O functions to eliminate parameters that were poorly estimated by the fit. This included parameters from (a) functions that were flat (<5 dB amplitude growth across all stimulus levels), (b) those that were flat across all stimulus levels except the highest level, at which a steep upswing in OAE level occurred, causing the maximum slope to be estimated at 65–75 dB, and (c) those where OAE amplitude was <–20 dB across all stimulus levels (i.e., it was flat and in the noise). Some 14% of total I/O functions were eliminated by these rules.

3. Receiver operating characteristic (ROC) curves

Clinical decision theory, a statistical framework for describing the accuracy with which a given test can achieve the goal of separating two populations based on a disease or other characteristic (Swets, 1988; Swets and Pickett, 1982), was applied to assess how well OAE metrics could distinguish between ears with impaired or normal hearing. Performance in the classification task was quantified and summarized using receiver operating characteristic (ROC) curves which plot the true-positive rate or hit rate (sensitivity) as a function of the false-positive (1-specificity) rate. At each test frequency, we constructed ROC curves for a variety of binomial logistic regression models, each employing one (or more) of the observed OAE metrics as independent variables. The models, implemented using MATLAB's `fitglm` function, were trained to predict the probability that the observations arose from an impaired (rather than a normal) ear, as defined by the audiogram.

Model training and cross-validation proceeded in two steps. First, for each metric we constructed 300 resampled data sets by random sampling (with replacement) from the ears contributing data at each test frequency. The resampled data sets were split into two halves; the model was then trained on the first half and tested on the second. Training and testing were repeated for each of the 300 data sets. Confidence intervals for the distribution of ROC curves obtained during this first step are shown in Fig. 2 as gray × symbols and gray vertical bars. In the second step, we improved the model generalizability (i.e., reduced any dependence on the possible idiosyncrasies of particular data sets) by averaging the coefficients for each of the 300 models (after removing possible outliers) to obtain a *mean* model. The mean model was then evaluated by testing it on the original data set, producing the final ROC curve shown by the black line in Fig. 2. This curve was validated by computing confidence bands on model performance (see magenta vertical bars) using additional resampled data sets.

III. RESULTS

Figure 3 shows individual DPOAE (top row) and SFOAE (bottom row) levels for the 40 dB FPL stimulus condition, plotted as a function of corresponding audiometric thresholds. Although eight audiometric thresholds were measured, only four are shown in Fig. 3 to illustrate the relationship between OAEs and hearing across frequency. These scatter plots were fit with a linear regression to probe the strength of the associations. As can be seen, DPOAE levels always correlate more strongly with audiometric thresholds than do SFOAE levels. Also, the best correlation is seen at 4 kHz where hearing thresholds account for 81% of the variance in DPOAE level. For SFOAEs, the correlation is equally strong at 2 and 4 kHz (0.80, 0.81), where audiometric thresholds account for up to 66% of the variation in SFOAE levels. These data, as well as past publications showing similar analyses (Gorga *et al.*, 1993a; Gorga *et al.*, 1993b; Gorga *et al.*, 1997), attest to a systematic relationship between audiometric thresholds and OAE levels.

A. OAE spectra

Figure 4 displays fine-resolution SFOAE and DPOAE spectra in one normal-hearing individual, for the full range of frequencies and stimulus levels. Each line consists of 500 points across the nearly five-octave range (100 points per octave). The SFOAE shows characteristic macrostructure including peaks and valleys, which are intrinsic to the

31 October 2024 19:47:36

https://doi.org/10.1121/10.0030399

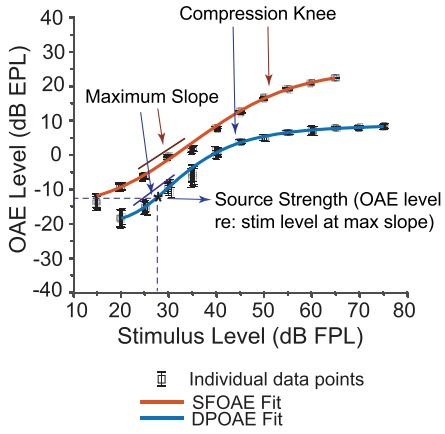

FIG. 1. (Color online) Example SFOAE and DPOAE input/output functions from one ear. The black open-square symbols are the data points, which are characterized with a least squares fit shown as red (SFOAE) and blue (DPOAE) lines. Three parameters (labeled) were derived from this fit to quantify the growth slope and compressive features of each emission.

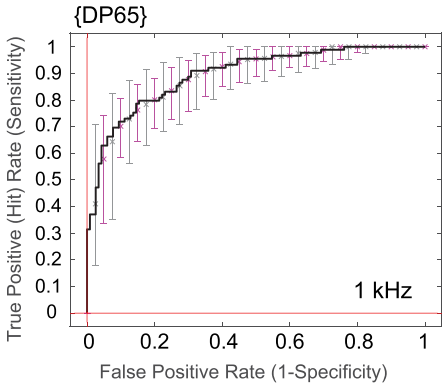

FIG. 2. (Color online) Example ROC curve and 95% confidence intervals illustrate the results of training and cross-validating one of the binomial logistic regression models. ROC curves plot true hit rate as a function of the false-positive rate. In this example, the regression model was trained using the value of a single OAE variable (DPOAE level at 1 kHz for 65 dB FPL) to classify ears as either normal hearing or hearing impaired at that frequency. The gray symbols (×) and gray vertical bars give the mean values and confidence intervals for the distribution of ROC curves obtained during the first training step, which involved 300 resampled data sets. In the second step, the mean model obtained during the first was tested on the original data set, producing the final ROC curve (seen as a black line). To obtain confidence bounds for this curve, the mean model was tested on an additional 300 resampled data sets (magenta symbols and confidence intervals).

reflection process. The DPOAE shows little fine structure because it includes only the separated nonlinear-distortion component, hence there is little or no residual component interference. This broad parametric space was covered for every ear tested (though the number of stimulus levels presented varied slightly depending on the degree of hearing loss).

Figure 5 shows simplified mean band-averaged spectra for each group and OAE. SFOAE and DPOAE level data points have been binned into half-octave-wide frequency bands defined by their center frequency. These group mean spectra are shown for probe and L_2 levels of 40 dB ($L_1 = 55$ dB) and 65 dB ($L_1 = 65$ dB) FPL. Data from the NH group is depicted by a red X for SFOAEs and a blue circle for DPOAEs. Consistent with a recent publication (Abdala *et al.*, 2022), below 2 kHz the mean SFOAE at 40 dB FPL is slightly higher in level than the corresponding DPOAE while above 2 kHz, the mean DPOAE is higher in level. At 65 dB FPL, mean SFOAE level is higher than DPOAE level (by as much as 15 dB) across the frequency range.

The group mean data from the HI group retain the same symbol code but we have used black for the SFOAE and gray for the DPOAE in this group. The dominant effect of mild hearing loss on OAEs is to reduce emission levels. At 40 dB FPL, the mean reductions approximate 20–25 dB at some frequencies and OAE reductions are greater for the DPOAE than the SFOAE. This becomes more apparent when "OAE loss" is calculated for the HI ears: OAE loss is defined as the OAE level in a HI ear subtracted from the mean OAE level of the normative group at the same frequency (i.e., the negative of the HI OAE level relative to normal). The DPOAE always showed larger OAE loss values than did the SFOAE, indicating a stronger impact of hearing loss on the distortion-product emission level. This same pattern has also been reported in aging cohorts (Abdala *et al.*, 2018a) and in those with endolymphatic hydrops (Stiepan *et al.*, 2023). At 65 dB FPL, the OAE loss metric was smaller than at 40 dB, which suggests that the lower stimulus level condition may be more effective in distinguishing the two groups.

OAE loss was analyzed in the HI group with a two-factor ANOVA: OAE (DP, SF) × frequency (1, 2, 4, 8 kHz). We were interested in the OAE factor to determine whether the two emissions were differentially affected by hearing loss. At both levels, ANOVAs showed main effects of OAE (40 dB: $F = 70.05$; $p < 0.001$; 65 dB: $F = 83.78$; $p < 0.001$) as well as interactions between OAE and frequency; *post hoc* analyses showed that SFOAEs and DPOAEs differed in OAE loss at 2, 4, and 8 kHz.

B. OAE input/output functions

The left column in Fig. 6 shows all I/O functions from normal hearers for three combined frequency bands: low frequency (0.75, 1, 1.5 kHz), mid-high frequency (2, 3, 4 kHz), and high frequency (6, 8 kHz). The thin colored lines are individual functions, and the thick red/blue lines are loess trend lines fit to the individual data. Briefly, SFOAEs are higher in level than DPOAEs at both low- and mid-frequencies; this difference becomes more pronounced with increasing stimulus level. At high frequencies, the two OAE levels are more similar. As evident, DPOAE growth is strongly compressive while SFOAE growth is less so. The right column of Fig. 6 shows the corresponding I/O functions for the HI group. In ears with hearing loss, the SFOAE is higher in level than the DPOAE for all frequency bands, again underscoring the fact that DPOAE levels are more reduced by hearing impairment than are SFOAE levels.

31 October 2024 19:47:36

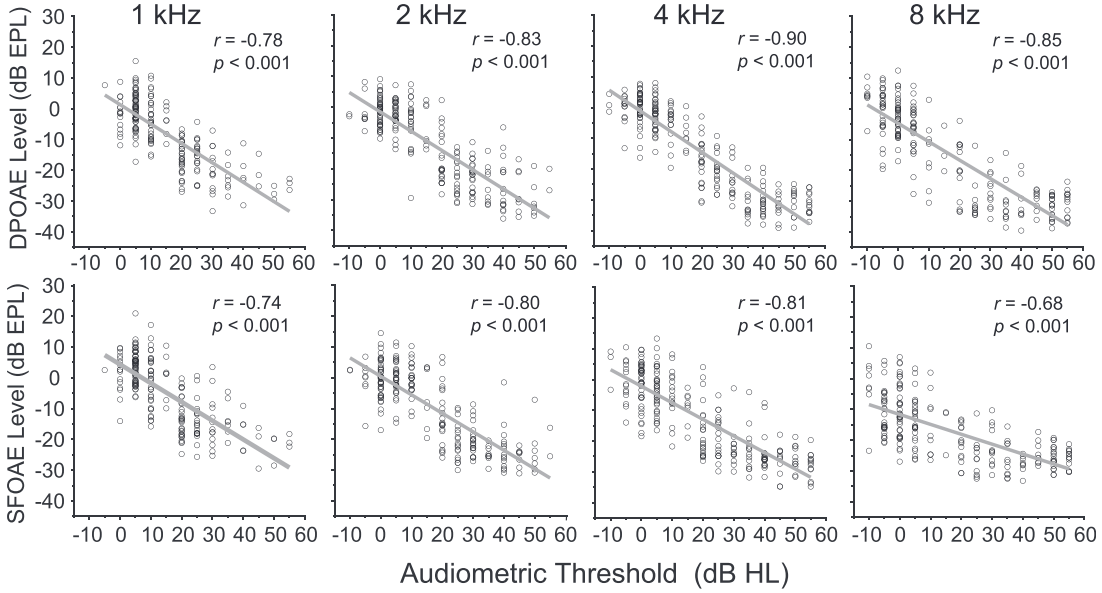

FIG. 3. DPOAE (top row) and SFOAE (bottom row) levels for four half-octave-bands centered at 1, 2, 4, and 8 kHz plotted as a function of audiometric threshold. Note that only target audiometric thresholds (20–55 dB HL) were included for HI ears. A regression line was fit to each plot and the r values for each correlation are provided. All correlations were significant at $p < 0.001$. While a systematic relationship was present for both OAEs, overall, correlations between OAE level and audiometric threshold were stronger for the DPOAE.

SFOAE amplitude appears to be more reduced at low (vs high) stimulus levels, producing a steepened growth slope in impaired ears.

Figure 7 displays the group mean values for the three parameters derived from fits to individual I/O functions across center frequency: maximum slope (dB/dB), source strength (dB), and compression knee (dB FPL). The left column shows data from the normal-hearing group as a reference. In healthy ears, the maximum slope of OAE growth hovers around 1 dB/dB for both emissions; source strength is equivalent for the two OAEs through ~3 kHz (beyond which it becomes stronger for the DPOAE); and the compression knee occurs at substantially higher stimulus levels for the SFOAE than DPOAE.

The corresponding mean data from ears with hearing loss are depicted in the right column of Fig. 7. Mild hearing loss produces disruptions in the three I/O function parameters and, in doing so, creates systematic shifts in the SFOAE-DPOAE relationship. Hearing-impaired ears show (1) steepened maximum slope for the SFOAE only, (2) overall reduced source strength for both OAEs, but more so for the DPOAE, and (3) elevated compression knee for the DPOAE, which acts to extend its linear range. The relative DP-SF differences in maximum slope, source strength, and compression knee were calculated as ΔMS, ΔSS, and ΔCK, respectively for the two subject groups, and each of these difference metrics was tested with a two-factor ANOVA: group (NH, HI) × frequency (1, 2, 4, 8 kHz). We were particularly interested in the *group* effect on

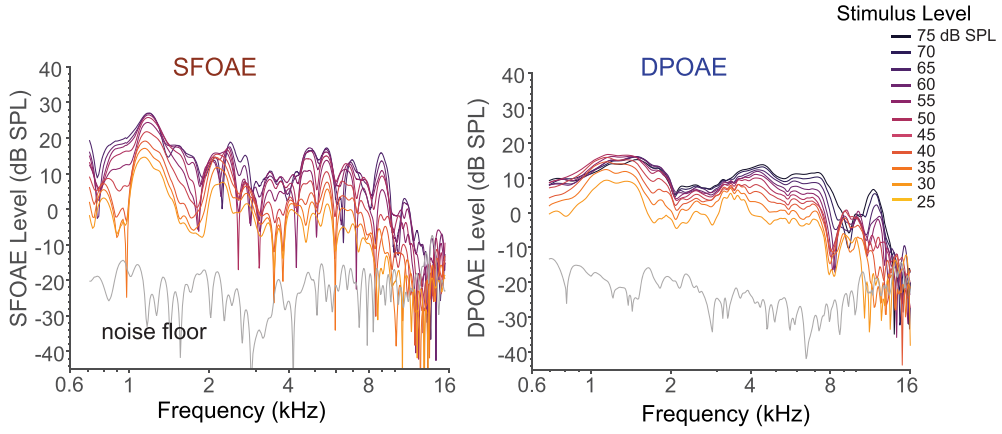

FIG. 4. (Color online) A level series of fine-resolution spectra for the SFOAE and the nonlinear-distortion component of the DPOAE from one healthy ear. 500 data points across frequency comprise each spectrum, and color denotes stimulus level. For reference, the gray line is the noise floor obtained for a mid-level stimulus. Unlike the spectral structure of the OAEs, which have adequate SNR, the spectral structure of the noise is not reproducible.

31 October 2024 19:47:36

https://doi.org/10.1121/10.0030399

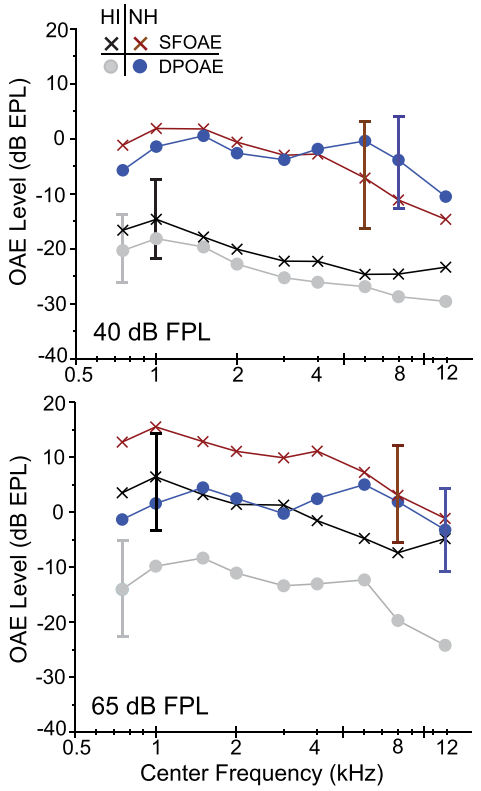

FIG. 5. (Color online) Group mean OAE level binned into half-octave bands denoted by center frequency for SFOAEs (red ×) and DPOAEs (blue ○) in the normal hearing group, and for SFOAEs (black ×) and DPOAEs (gray ○) in the hearing-impaired group. Data are shown at two stimulus levels: 40 and 65 dB FPL. Standard deviations were relatively constant across frequency hence, to minimally obscure trends, only one error bar (2 standard deviations) is plotted per group and OAE.

the DPOAE-SFOAE metric because it addresses whether hearing loss impacts reflection and distortion emissions differently. ΔMS starts out near 0 in normal-hearing ears since the growth slopes are roughly equivalent for SFOAEs and DPOAEs, however, in HI ears, the steepened growth of the SFOAEs, combined with negligible changes in DPOAE growth, produces a significant group effect in ΔMS [$F = 304.1$; $p < 0.001$; see Fig. 7(A) vs 7(D)]. The ΔSS metric also showed a significant effect of group ($F = 390.1$; $p < 0.001$): In hearing-impaired ears, the source strength becomes relatively stronger for the SFOAE (vs DPOAE) across all frequencies [Fig. 7(B) vs 7(E)]. Finally, ΔCK showed a significant group effect as well ($F = 266.49$; $p < 0.001$): In normal ears, SFOAEs compress at higher stimulus levels than do DPOAEs; however, with hearing loss, the DPOAE compression knee increased by as much as 20–25 dB whereas SFOAE compression changed only slightly [see Fig. 7(C) vs 7(F)]. *The significant effect of hearing loss on these three DP-SF difference metrics suggests that cochlear injury impacts distortion and reflection emissions differently.*

C. OAE classifiers

The effect of hearing loss on SFOAE and DPOAEs (as shown in Figs. 5–7) provided guidance on which OAE variables were likely to be most effective in classifying ears correctly. We constructed classifiers using both single OAE metrics and sets of OAE metrics as independent variables. To ensure that we did not miss any potent combinations, we employed forward stepwise regression (as implemented in MATLAB's `stepwiseglm` function) to iteratively construct the regression model by sequentially including additional independent variables (OAE metrics) that yielded statistically significant increases in performance. Although the results of the stepwise regression varied somewhat across frequency, it consistently identified many of the same metrics as our observations.

To display examples of resulting ROC curves, we show two classifiers that performed well across frequency in Fig. 8. The black line shows the mean model ROC curve for each condition and classifier. The first classifier (right column) combines two OAE variables {DPSS, SFSS}; the second (left column) combines four variables {DP40, SF40, DPCK, SFMS}. Variable abbreviations and definitions are provided below Table I. The gray band around each ROC curve consists of 300 thin lines, each representing a curve obtained by training the model on 300 artificial data sets generated by random resampling. While the area under the curve is one measure of overall model performance, it does not provide a metric tied to a specific false-positive rate. We therefore chose to compare hit (or true-positive) rates at selected false-positive rates to assess performance.

A larger group of 12 variable sets for which ROC curves were generated is shown in Table I. In Table I, the top half of Table I presents hit rate (with a 10% acceptable false positive rate) across center frequency. The bolded variable sets are those that performed best. The key linking variable number with a corresponding OAE variable set is provided in the bottom half of the table. The SFOAE alone (at any stimulus level or for any I/O-function-derived variable) did not produce strong hit rates, as exemplified by variables #2 and #6. However, SFOAE information enhanced hit rates *when combined with the DPOAE*, as exemplified by variable set #4, which produced hit rates of between 91% and 98% across the entire frequency range. Also, evident is that OAEs measured using low-level stimuli (40 dB FPL) always performed better than those evoked at higher levels (65 dB FPL). This can be seen when comparing hit rates for variable sets #1 vs #3. I/O-function parameters used alone did not classify ears with high hit rates across all frequencies, as evidenced by variable sets #5 and #6, where DPOAE compression knee and SFOAE maximum slope failed to detect hearing loss well, in particular at low-mid frequencies. However when SFOAE slope and DPOAE compression knee were combined with measures of OAE level at 40 dB FPL, they produced some of the strongest hit rates observed across frequency (variable set #7). Naively, it might seem that simply adding *more* information to a classifier should always produce better hit rates. However, a closer look indicates that using *more* OAE metrics did not guarantee strong performance. Variable set #9 in Table I includes both DPOAE and SFOAE levels at 65 and 40 dB, respectively, but does not perform as well as do variable sets #1 or #10 that include only one OAE metric.

31 October 2024 19:47:36

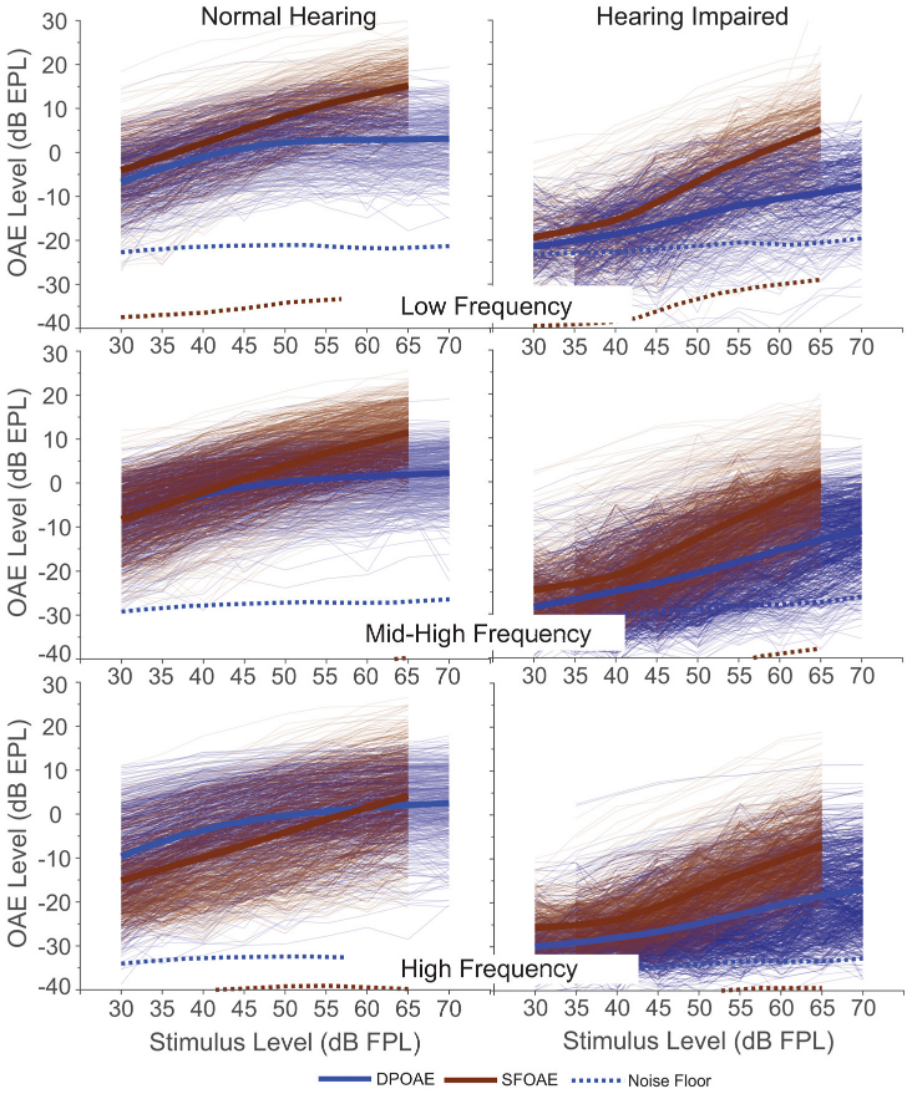

FIG. 6. (Color online) Individual input/output functions are displayed (as thin red and blue lines) and loess trend lines (thick) are fit to these data. The functions are shown within three frequency bands as labeled: low-frequency, mid-high frequency, and high-frequency. Mean noise floors are shown as dotted lines.

Unsurprisingly, it is the quality (or relevance) not the quantity of the information that matters.

Figure 9 plots hit rates (with 10% and 5% false positives) for five of the best classifiers. With a fixed false positive rate of 10%, the OAE variable sets in Fig. 9 that achieved 90% or better across all nine center frequencies were {SF40, DP40} (filled circles) and {SF40, DP40, SFMS, DPCK} (open circles, dashed line). Others achieved 90% or better at all but one or two frequencies {DPSS} and {DPSS, SFSS}. Note that combining SFOAE level with DPOAE level at 40 dB improves hit rates (re: the DPOAE alone) for the lowest frequency band (0.75 kHz). This can be visualized by comparing the filled circle to the open square.

When the acceptable false positive rate is stricter (5%, see bottom panel), it reduces hit rates overall. However, the advantage of including SFOAE together with DPOAE metrics becomes stronger. For example, DPOAE source strength (SS) classifies ears with sensitivity of $\geq 90\%$ at most frequencies when a fixed false positive rate of 10% is used (top panel) and including SFOAE SS does little to improve sensitivity (note superimposed triangle and X symbols). However, with a fixed false positive rate of 5% (bottom panel), using both SFOAE SS and DPOAE SS together shows better performance at some frequencies than does the DPOAE SS alone (note the triangle above the X symbol). Recall that nearly 80% of impaired thresholds are in the slight-to-mild range of hearing loss. Hence, our best results are achieving hit rates of 91–99% for the detection of the most challenging and most frequently missed hearing losses.

D. Factors influencing improvement

In this study, the swept-tone joint-OAE profile showed clear improvements over early work exploring the clinical utility of OAEs (see bolded hit rates in Table I vs the summary of hit rates for past literature presented in the Introduction). In Fig. 10 we examined some of the methodological differences that could have contributed to this improvement. To do this, we re-analyzed our OAE amplitude data using alternative methods, and contrasted these hit

31 October 2024 19:47:36

https://doi.org/10.1121/10.0030399

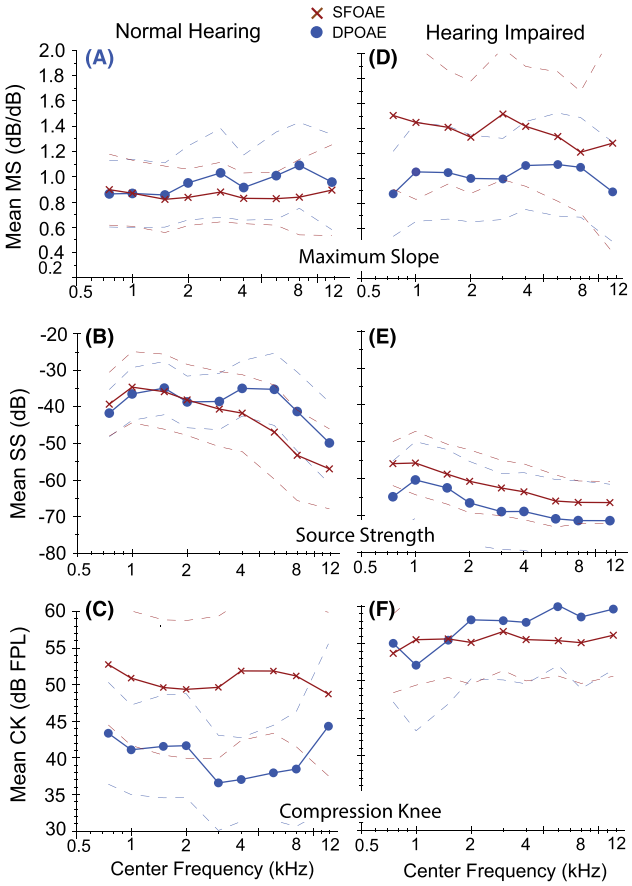

FIG. 7. (Color online) (A)–(F) Three parameters are derived from a fit to the I/O functions and plotted as a function of center frequency: maximum slope [(A) and (D)], source strength [(B) and (E)], and compression knee [(C) and (F)]. Mean data from the normative group are shown in the left column and from hearing-impaired group, in the right column for corresponding parameters. SFOAEs are shown in red and DPOAEs in blue. The thin dashed lines represent 2 standard deviations. The I/O function parameters are altered by hearing loss in three basic ways (compare like parameters in left and right columns): SFOAE slope steepens, source strength weakens (more so for the DPOAE than SFOAE), and the compression knee is elevated for the DPOAE.

rates with those achieved by one classifier in the current joint protocol, DP40, SF40. These re-analyzed results do not exactly simulate past work because many methodological factors could not be recreated or manipulated *a posteriori* nor can they disentangle the contributions of each factor to performance. The primary three factors examined were (A) analyzing the OAE at a single test frequency (vs analysis within a half-octave frequency band comprised of ∼50 frequency points), (B) analyzing the total DPOAE (vs only the separated nonlinear distortion component of the DPOAE), and (C) Imposing a 6 dB-SNR criteria for the inclusion of DPOAE data (vs our non-elimination of any data based on SNR). In all panels, analysis of the DPOAE-alone was compared to our *joint* reflection-distortion approach.

The filled purple circles in Figs. 10(A) and 10(B) represent hit rates for one of the top classifiers, {DP40, SF40}, using our current joint protocol. Hit rates of 91%–98% are achieved across frequency with this variable set. In panel (A), the orange x symbol depicts hit rates derived from the same group of ears when the distortion component of the DPOAE was measured and analyzed at a single test frequency (not within a frequency band). This single-frequency analysis method yields much-reduced hit rates (∼ 50% at the lowest and highest test frequencies). The best performance achieved is 82% at 8 kHz. When SFOAE level at 40 dB, also analyzed at a single frequency, is combined with the DPOAE, hit rates improved to some extent, although they are still lower than those achieved by utilizing a frequency-band analysis (orange triangle).

Figure 10(B) shows a comparison between our current protocol using variable set {DP40, SF40} and the total unseparated DPOAE (analyzed in every other way as in our current protocol). Utilizing the total DPOAE at 40 dB (orange X symbol) reduces sensitivity to hearing loss greatly at frequencies < 2 kHz but one can compensate by including SFOAE level (see orange triangles). The hit rates remain slightly below those of our current protocol, but substantial improvement is obtained by including the SFOAE; sensitivity ranges from 82% to 92% when both OAEs are considered together, even though the DPOAE is unseparated.

Figure 10(C) illustrates the impact of using SNR-based criteria to eliminate OAEs that are close to the noise floor. We could not conduct re-analysis at 40 dB FPL because implementing SNR-based criteria eliminates too much data at the lower stimulus level. Hence, the comparison was done at 65 dB FPL, which reduced hit rates overall. The open purple circles show hit rates for the current protocol, variable set {DP65, SF65}. For comparison, the DPOAE in this re-analysis was the total, unseparated DPOAE. As evident, sensitivity to hearing loss was degraded whenever SNR-based criteria were imposed, in particular, for frequencies < 4 kHz (see orange triangle and × symbols). Also, evident is that, at this higher stimulus level little improvement is gained by including the SFOAE.

It is also likely that using FPL-based stimulus calibration and the EPL correction to OAE level, both techniques that mitigate the effect of ear-canal standing waves on OAE measurements, contributed to improved hit rates. These techniques are known to produce more reliable and stable behavioral thresholds and OAE measurements (Scheperle *et al.*, 2011; Reuven *et al.*, 2013; Souza *et al.*, 2014; Maxim *et al.*, 2019). However, because the stimulus calibrations could not be manipulated *a posteriori*, we were unable to test the specific influence these methods may have had on the detection of mild hearing loss.

E. Results summary

A consistent pattern of OAE abnormalities emerged when emissions were measured in slight-to-moderately impaired ears. Hearing loss produces a triad of disruptions: (1) It reduces OAE amplitude and source strength, more so for the DPOAE than the SFOAE, (2) it steepens the SFOAE growth slope by reducing OAEs evoked by low-level stimuli more than those evoked by

31 October 2024 19:47:36

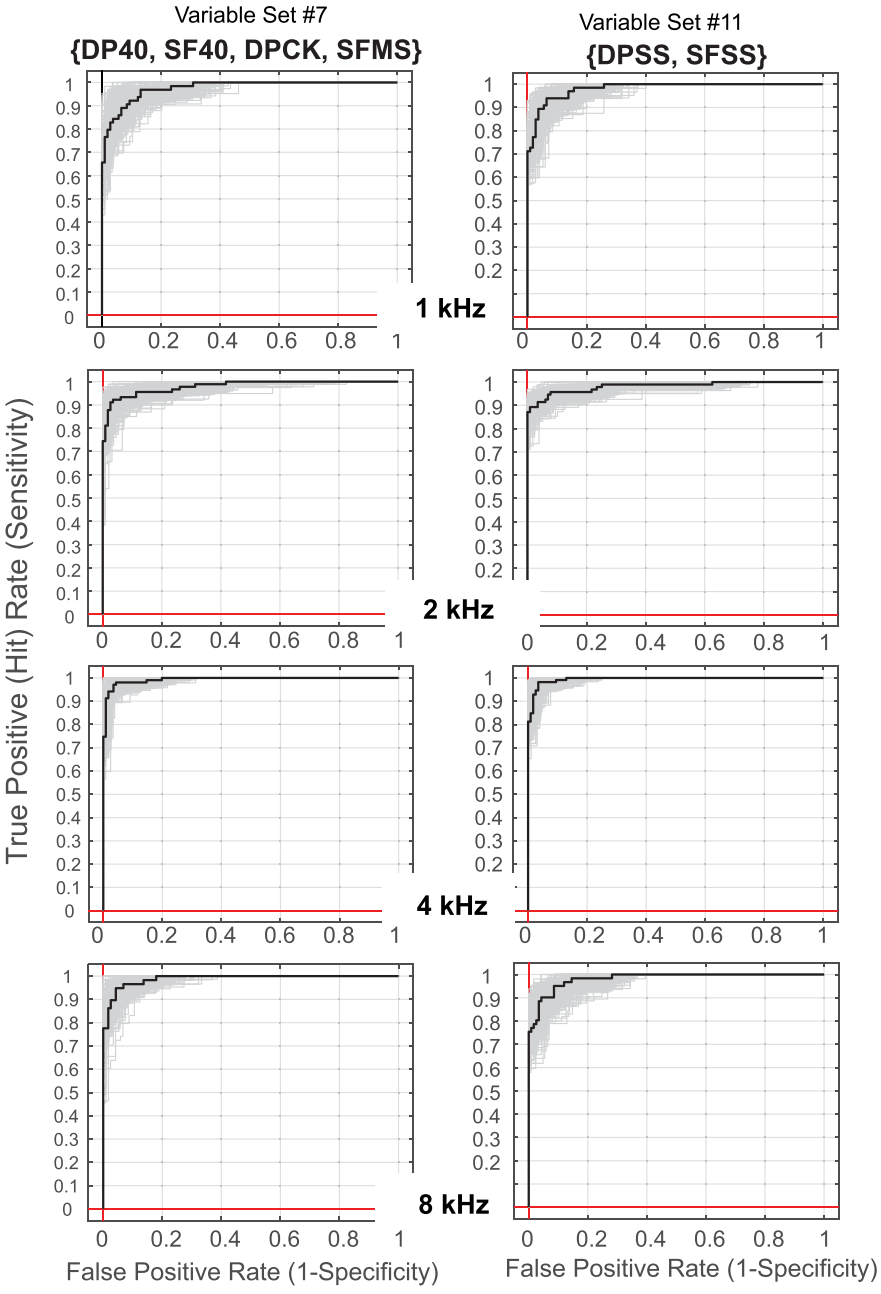

FIG. 8. (Color online) Receiver operating characteristic (ROC) curves (black lines) summarizing the performance of the mean model in classifying ears as either normal hearing or hearing impaired for two exemplar OAE variable sets. True hit rate is plotted as a function of false positive rate. The shaded gray area was generated by resampling 300 additional OAE data sets (with replacement); the 95th % confidence intervals in Table I were calculated from this resampling. Four test frequencies are shown here. The left column displays performance for a variable set combining SFOAE and DPOAE levels evoked at 40 dB FPL with SFOAE maximum slope (MS) and DPOAE compression knee (CK). The right column displays performance for a variable set combining the source strength (SS) of both DPOAE and SFOAE. By fixing an acceptable false positive rate on the x axis one can intersect the ROC curve on the y axis and determine the performance (hit rate) of any given variable set in classifying an ear as normal hearing or hearing impaired.

high levels, and (3) it pushes the compression knee of the DPOAE toward higher stimulus levels, effectively extending its linear range. *Mild hearing loss systematically alters the relationship between reflection and distortion emissions, suggesting that the two emission classes have distinct sensitivities to cochlear pathology and dysfunction.* Using our best OAE classifiers, the swept-tone Joint-OAE profile was able to detect mild hearing loss with hit rates of 92–99% at center frequencies from 0.75 kHz to 12 kHz. The results reflect strongly improved performance relative to previously published reports using conventionally measured/analyzed OAEs in the detection of hearing loss. One contributor to this enhanced performance is the inclusion of data from both distortion and reflection OAEs combined.

IV. DISCUSSION

Mild hearing loss impacts reflection and distortion emissions differently, suggesting distinct sensitivities to cochlear pathology; this distinct behavior appears to improve the detection of mild hearing loss and supports the strategy of using a joint-OAE approach to diagnostics. The joint-OAE profile, which is meant to access and exploit dual cochlear processes involved in the generation of DPOAEs and SFOAEs, detected mild hearing loss with high sensitivity ($\geq$90%) across almost five octaves. Combined, these two classes of OAEs—namely, the distortion component of the DPOAE, which is thought to probe the strength and form of the cochlear nonlinearities, and the SFOAE, a reflection emission linked to cochlear amplifier gain and tuning—were

31 October 2024 19:47:36

https://doi.org/10.1121/10.0030399

TABLE I. Hit rate (with fixed 10% false positives) across nine center frequencies. The values in the brackets represent 95% confidence intervals generated through resampling (see Sec. II). The bolded OAE variable sets are those that performed best across frequency.

	Center frequency (kHz)								
OAE variable set #	0.75	1	1.5	2	3	4	6	8	12
1	**88** [79–100]	**92** [81–98]	**97** [90–100]	**93** [88–98]	**92** [87–98]	**97** [90–100]	**98** [94–100]	**92** [87–99]	**97** [84–100]
2	85 [74–96]	84 [70–92]	90 [84–97]	92 [81–97]	82 [75–90]	86 [78–94]	81 [68–90]	69 [49–88]	57 [46–80]
3	72 [57–85]	72 [60–82]	74 [56–86]	80 [70–89]	80 [72–89]	84 [72–93]	91 [83–96]	92 [86–97]	92 [86–98]
4	**95** [91–100]	**91** [81–99]	**97** [91–100]	**94** [87–99]	**92** [88–98]	**97** [92–100]	**98** [92–100]	**92** [84–99]	**97** [86–100]
5	67 [33–88]	67 [49–85]	72 [54–88]	90 [82–97]	99 [94–100]	97 [92–100]	96 [90–100]	94 [84–99]	78 [54–89]
6	60 [42–79]	69 [53–80]	77 [57–87]	77 [64–87]	81 [49–90]	83 [75–91]	83 [68–90]	57 [33–72]	48 [37–64]
7	**97** [91–100]	**92** [81–100]	**96** [91–100]	**93** [89–99]	**99** [94–100]	**98** [95–100]	**99** [94–100]	**97** [91–100]	**95** [81–100]
8	**97** [84–100]	**94** [76–99]	**96** [88–100]	**95** [86–99]	**100** [90–100]	**98** [95–100]	**99** [95–100]	**95** [88–100]	**92** [77–100]
9	91 [80–99]	87 [74–94]	91 [84–97]	92 [84–97]	86 [78–92]	90 [85–98]	95 [87–99]	93 [84–98]	95 [86–99]
10	**97** [85–100]	**92** [85–99]	**96** [84–100]	**96** [89–99]	**98** [94–100]	**98** [95–100]	**98** [94–100]	**95** [83–100]	**83** [67–95]
11	**100** [89–100]	**94** [86–100]	**96** [89–100]	**96** [90–99]	**98** [94–100]	**99** [96–100]	**99** [96–100]	**95** [84–100]	**85** [74–98]
12	**100** [94–100]	**94** [86–100]	**96** [86–100]	**96** [90–99]	**99** [96–100]	**97** [95–100]	**98** [95–100]	**100** [92–100]	**88** [76–98]

#	**OAE Variable Sets**
1	**DP40**—DPOAE level at 40 dB FPL
2	SF40—SFOAE level at 40 dB FPL
3	DP65—DPOAE level at 65 dB FPL
4	**DP40, SF40**—DPOAE and SFOAE level at 40 dB FPL
5	DPCK—DPOAE compression knee
6	SFMS—SFOAE maximum slope
7	**DP40,SF40, DPCK, SFMS**—Variable set #4, #5 and #6 combined.
8	**DP40, DPCK**—Variable set #1 and #5 combined
9	DP65, SF40—Variable set #2 and #3 combined
10	**DPSS**—DPOAE source strength
11	**DPSS, SFSS**—DPOAE and SFOAE source strength
12	**DPSS, SFMS**—Variable #6 and #10 combined

able to detect mild hearing loss with outstanding accuracy. These findings prompt the continued exploration and development of a joint-OAE approach to hearing diagnostics with the future goal of differential diagnosis (i.e., distinguishing between two ears with similar degrees of hearing loss but distinct etiologies). The clinical practice of arbitrarily measuring one of the two OAE types (either DPOAEs or transient-evoked OAEs typically) when testing patients for hearing loss is not supported by our results. Nor do our results support the continued use of conventional *discrete-tone* OAE measurement in individuals with suspected hearing loss because their speed, efficiency, and resolution cannot match that offered by swept-tone stimuli.

A. Basilar-membrane motion

Mild sensory hearing loss produced a reliable triad of disruptions in OAE growth and compression. This profile of OAE abnormality was consistent with what has been reported from direct basilar-membrane measurements in laboratory animals with induced cochlear injury [e.g., Rhode (1971), Ruggero and Rich (1991), and Robles and Ruggero (2001)]. OAEs from the impaired cochlea show reduced responses (i.e., reduced gain) with steepened and less compressive growth. Chinchillas exposed to furosemide, which blocks OHC transduction by reducing the endocochlear potential, show smaller displacements of the basilar membrane consistent with reduced gain; this reduction is more pronounced for low- vs high-level stimuli, which steepens the growth function. Furthermore, basilar-membrane responses in a healthy cochlea grow compressively near the best frequency but become linearized when damage is induced (Ruggero and Rich, 1991). The joint-OAE profile roughly mirrors the response of the basilar membrane when the cochlea has been compromised.

B. Comparisons with other work

There were some fundamental differences between our methods and those in previously published reports. One stark difference is that past studies used only one of the two classes of OAEs to detect hearing losses, never reflection and distortion emissions together. Here, some of our best classifiers across frequency included metrics derived from both classes of emissions combined, such as the SFOAE and DPOAE level at 40 dB FPL, as well as these level measurements combined with the maximum slope of the SFOAE growth function and the compression knee of the DPOAE. These two variable sets produced $>90\%$ hit rates across all center frequencies, from 0.75 to 12 kHz. Our hypothesis is that we are accessing two distinct generation mechanisms and exploiting the information that each offers about cochlear integrity with our joint-OAE profile. Results confirmed that mild hearing loss impacts these two emissions in

31 October 2024 19:47:36

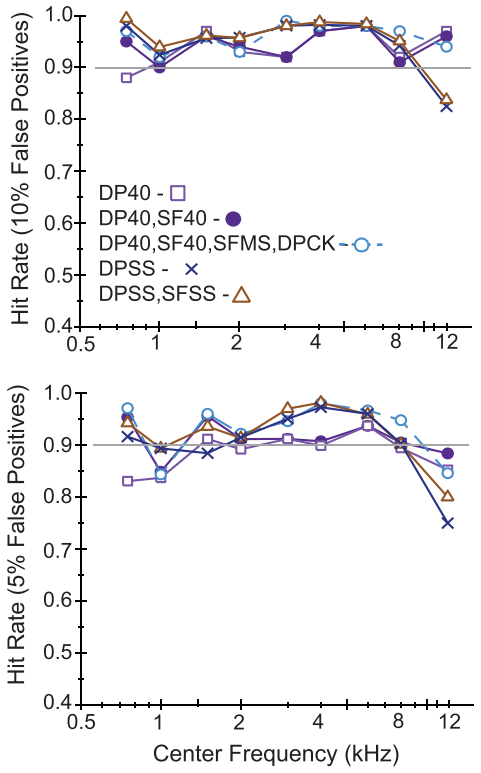

FIG. 9. (Color online) Hit rate (with fixed false positive rates of 10% and 5%) for five of the top OAE classifiers. A line is drawn at 90% to highlight that two variable sets in this figure achieved ≥ 90% across all center frequencies: {SF40, DP40} and {SF40, DP40, SFMS, DPCK} (see Table I for definitions of OAE variables). When a stricter acceptable false positive rate is applied (bottom panel), sensitivity is slightly reduced as expected.

distinct ways (see Fig. 7), and so it is not surprising that using them together might synergistically enhance the detection of hearing loss. When these signature distortion and reflection OAE sensitivities are combined, they detect mild hearing loss with strong accuracy across all nine frequencies. The detection of mild hearing loss was most notably improved in the low-to-mid frequencies when SFOAEs were combined with a DPOAE metric, supporting the notion that the two emissions each offer a slightly different "look" at cochlear hearing loss.

Another difference between our studies lay in the measurement of the DPOAE. Because a central purpose of the present study was to assess the value of exploiting OAE generation mechanisms, it was essential for us to separate the nonlinear distortion component of the DPOAE rather than analyze the total DPOAE, which leaves uncontrolled contributions from reflection components. Figure 10(B) suggests that not separating out the distortion component of the DPOAE reduced hit rates, particularly at low frequencies. The failure to control DPOAE components allows for component interference which produces spectral fine structure. When the total DPOAE is measured at single frequencies, the tester cannot know where along the fine structure pattern the chosen test frequency falls. When located at a deep minimum in fine structure, the resulting estimates of DPOAE amplitude may reduce its ability to detect hearing loss.

Johnson and colleagues (Johnson *et al.*, 2007; Go *et al.*, 2019) concluded that the impact of using the total DPOAE (vs the distortion-component only) was negligible when considering their *full* group of subjects; however, more substantive improvements were observed when focused on only the most mildly impaired ears in their group, at the lowest stimulus levels. This is consistent with the findings here in our mostly slight-to-mildly impaired subjects at 40 dB FPL. Detecting hearing loss in a subject cohort with moderate or moderate-severe hearing loss may be nearly equivalent for the total DPOAE vs separated distortion component because greater degrees of hearing loss are more easily detected; the difference may be negligible. However when attempting to

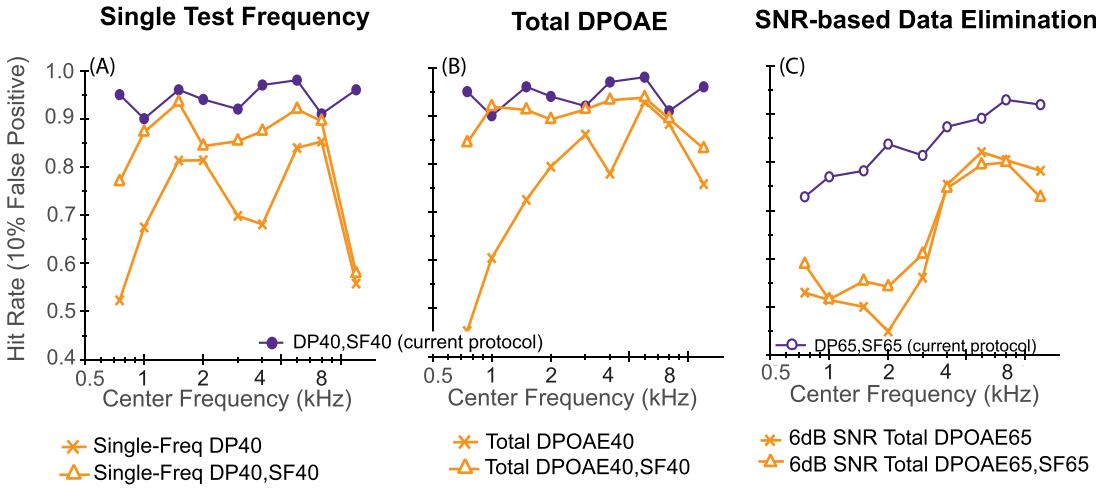

FIG. 10. (Color online) (A)–(C) The effects of frequency-band analysis, DPOAE unmixing, and SNR-based data elimination on hit rates. Panel (A) shows comparisons between the current protocol (purple filled circles) that is analyzed as a frequency band and DP40 analyzed at a single test frequency (orange X); panel (B) shows comparisons between the current protocol, which analyzes the separated distortion component of the DPOAE and the total DPOAE (orange X); and panel (C) compares the current protocol (at 65 dB, open circles), which retains all OAE data vs the total DPOAE analyzed with SNR-based data elimination (orange x). Additionally, all comparisons illustrate the effect of including the SFOAE on performance (orange triangle) vs utilizing the DPOAE alone.

31 October 2024 19:47:36

detect the more difficult cases (i.e., ears with slight-to-mild amounts of hearing loss), our findings indicate that the separation of the DPOAE distortion component is influential and improves sensitivity. Others have also reported that separating the DPOAE produces more reliable estimates of audiometric threshold (Zelle *et al.*, 2017b).

A third difference between current and past studies is that the joint-OAE protocol included up to 50 data points in a half-octave frequency band, which was our unit of analysis, rather than a single data point at one test frequency. Reanalyses of OAE data to mimic single-frequency methods [see Fig. 10(A)] suggests that the frequency-band approach produces better hit rates than does an OAE analyzed at a single test frequency, as conventionally applied. The problems encountered when using single test frequencies are exacerbated by failing to separate the distortion component of the DPOAE because the single test frequency may fall on a non-ideal segment of DPOAE fine structure (i.e., a minimum or flank of a fine structure period). Of the early studies investigating clinical utility of OAEs, the analyses that performed best in detecting hearing loss applied multivariate approaches [Hussain *et al.* (1998), Dorn *et al.* (1999), and Gorga *et al.* (2005)]. By including predictive information across several frequencies combined, multivariate approaches achieved the strongest hit rates reported among these early studies [e.g., Dorn *et al.* (1999)]. This strategy most approximates the concept of a frequency band; that is, including more correlated frequency information appears to strengthen the detection of hearing loss.

One striking and salient contrast between this study and those conducted nearly 30 yrs ago is that here, the use of low- (rather than moderate-high) level stimuli unequivocally achieved the strongest hit rates. As evident from the mean data shown in Figs. 5 and 10 and Table I, the 40 dB stimulus level more effectively separated impaired and normal-hearing individuals. Others have reported that aging-related declines in hearing are observed earlier using DPOAEs evoked at low-moderate levels (25–45 dB SPL) (Glavin *et al.*, 2021) and that low stimulus levels also provided the greatest sensitivity to noise exposure (Poling *et al.*, 2022). This contrasts with the higher stimulus levels previously recommended for diagnostic assessment (Stover *et al.*, 1996). For decades the default stimulus parameters used to diagnose hearing loss with OAEs in the audiology clinic has been 65–55 dB or thereabouts. Our analysis indicates that L_2 and probe levels of 65 dB produced relatively poor hit rates compared to those obtained using lower-level stimuli.[2] In the present study, 40 dB FPL was often the lowest stimulus level presented to impaired ears; and the classifier variable set including both DPOAE and SFOAE levels at 40 dB FPL was one of the most potent variables. *These results unequivocally support the finding that moderate-high stimulus levels do not detect mild hearing loss as well as low levels*. This finding may be due to greater sensitivity of the low-level regime of auditory function, where the cochlear amplifier is actively impacting wave motion. At higher levels, OAEs are in the saturated portion of their growth and less responsive to the physiological changes induced by hearing loss. As a result, the mildest hearing losses may be missed when testing at high stimulus levels.

To optimize the apparent sensitivity of OAEs evoked by low-level stimuli, one must carefully consider how to deal with low level/low SNR data when characterizing OAEs. In contrast to some past studies using OAEs to detect hearing loss, we did not exclude low-level OAE data points that failed to meet SNR criteria; this does not benefit the accurate detection of hearing loss and is bad practice. It eliminates the very OAEs that are indicative of hearing loss and artificially skews group data toward higher amplitude OAEs. Recall that OAEs evoked by low-level stimuli performed best in the detection of hearing loss, yet OAEs evoked by 40 dB FPL in the current study would have been disproportionately eliminated by using SNR-based criteria. In this study, data points that had low SNR because the intracochlear signal was weak, were of interest; those that had low SNR because noise was excessive were not and they were eliminated. As a result, we could be confident that the retained OAEs, even those with low SNR, were mostly indicative of cochlear status. By retaining points close to the noise floor, we captured optimal indicators of hearing loss, which contributed to improved hit rates.

Other research groups have also had some success in applying advanced OAE methods for diagnostic and monitoring purposes, such as the use of pulsed stimuli which allows for rapid DPOAE component separation in the time domain [e.g., Zelle *et al.* (2017a), Zelle *et al.* (2017b), and Bader *et al.* (2024)]. The specific objectives of this promising work differ from our own in that they take a single-OAE (vs joint) approach, and their goal is to estimate behavioral thresholds. However, our larger goals are similar as their findings support DPOAE component separation, advanced calibration, and individually optimized parameters. A direct comparison with our work is not possible since the accuracy with which their method can detect mild hearing loss has not been assessed in a large cohort [see Zelle *et al.* (2017a)].

C. Detecting slight-mild hearing loss

Most of the seminal studies on OAE clinical utility cited in this report tested subjects with a wide range of hearing loss, including moderate-severe, severe, and profound hearing impairments. The greater the degree of loss, the more easily a classifier variable should be able to distinguish between impaired and healthy ears. The subject group in the present study had hearing loss ranging from slight to moderate but was dominated by slight-to-mild hearing loss—nearly 80% of thresholds were $\leq$ 40 dB HL and the overall mean audiometric threshold in the hearing-impaired group was 39 dB HL. Therefore, our task of classifying ears appropriately was more difficult because the contrast between the two cohorts was reduced. These slight-to-mild hearing losses are those most often missed in screening and diagnostic protocols and form the "false-negative" segment of the outcome matrix.

31 October 2024 19:47:36

Recent work as well as studies conducted decades ago (Bess, 1985; Bess *et al.*, 1998; Petley *et al.*, 2021) have reported negative educational, emotional, and social sequelae of even a slight degree of threshold elevation in children. What we once considered negligible hearing loss of little consequence is now recognized as an indicator of academic success and quality of life. The present study suggests that we can detect hearing loss in these slightly impaired ears with high accuracy and acceptable false positive rates, the latter of which may keep the cost of such a screening program reasonable. The present study was almost entirely comprised of adults older than 18 years of age. However, a follow-up study with some of the best OAE classifiers identified here could determine whether a joint-OAE profile in school-aged children would detect slight-to-mild hearing loss with the same high sensitivity we have found in adults. Catching slight-to-mild hearing loss early in these children could allow for remediation or academic accommodation as needed.

D. Future directions

Our research characterizing various aspects of the swept-tone Joint (reflection-distortion) OAE Profile in newborns, young and older adults, and individuals with ear disease (Abdala and Kalluri, 2017; Abdala *et al.*, 2018a; Abdala *et al.*, 2019; Abdala *et al.*, 2022; Stiepan *et al.*, 2023) support its utility in the lab and possibly in the clinic. Whether the improvements observed here (in analyzing both classes of OAEs together) will lead to an effective and abbreviated audiological test has not been established in the present study, and requires additional research. Applying swept tones for unparalleled frequency resolution and efficiency, using advanced calibration methods to mitigate standing wave inaccuracies, and exploiting two distinct classes of emissions combined, merit continued development and validation.

Ongoing work is currently probing the joint-OAE profile's ability to distinguish between ears with similar degrees but distinct etiologies of hearing loss. Other projects are investigating whether joint-OAE protocols using FPL stimulus calibration can monitor hearing effectively and provide earlier detection of hearing shifts upon repeated testing. These studies are critical for updating traditional OAE methods) (i.e., single-emissions, discrete-tone stimuli, static parameters, and abbreviated frequency and level ranges) and moving towards more comprehensive, advanced protocols. We see no reason why a researcher or clinician should use conventional but outdated methods and protocols for the measurement/analysis of OAEs, either for diagnostics or the study of cochlear function and dysfunction. Our hope is that commercial instrumentation will soon be developed to test and adopt some of the optimally effective protocols presented here to detect mild hearing loss.

ACKNOWLEDGEMENTS

This work was supported by Grant Nos. R01 DC018307 and T32 DC009975 from the National Institutes of Health. We thank Anusha Yellamsetty and Samantha Mohn for help with data collection during early segments of this project.

AUTHOR DECLARATIONS

Conflict of Interest

The authors have no conflicts to disclose. Informed consent was obtained from all subjects participating in this study according to the policies governed by the University of Southern California Institutional Review Board.

DATA AVAILABILITY

The data that support the findings of this study are available from the corresponding author upon reasonable request.

[1]We measure two independent OAEs vs unmixing of DPOAE components to access both reflection and distortion components, because the latter approach poses problems: (1) The reflection component makes a relatively small contribution to the total DPOAE and typically has low signal-to-noise ratio, in particular in hearing-impaired ears and when using the most common stimulus parameters, (2) reflection components can never be entirely or perfectly "unmixed" from the distortion component of the DPOAE and characterized in isolation (Abdala *et al.*, 2014); and, importantly, (3) there is no way to control or estimate the level of the stimulus evoking the reflection-component of the DPOAE, adding imprecision to measurements.

[2]It should be noted that our primary tones at 65 dB FPL have equal levels, as we followed the scissors method of establishing level separation: $L_1 = 0.4L_2 + 39$ dB SPL.

Abdala, C., and Dhar, S. (**2010**). "Distortion product otoacoustic emission phase and component analysis in human newborns," J. Acoust. Soc. Am. **127**, 316–325.

Abdala, C., and Dhar, S. (**2012**). "Maturation and aging of the human cochlear: A view through the DPOAE looking glass," J. Assoc. Res. Otolaryngol. **13**, 403–421.

Abdala, C., Guardia, Y. C., and Shera, C. A. (**2018b**). "Swept-tone stimulus-frequency otoacoustic emissions: Normative data and methodological considerations," J. Acoust. Soc. Am. **143**, 181–192.

Abdala, C., Guérit, F., Luo, P., and Shera, C. A. (**2014**). "Distortion-product otoacoustic emission reflection-component delays and cochlear tuning: Estimates from across the human lifespan," J. Acoust. Soc. Am. **135**, 1950–1958.

Abdala, C., and Kalluri, R. (**2017**). "Towards a joint reflection-distortion otoacoustic emission profile: Results in normal and impaired ears," J. Acoust. Soc. Am. **142**, 812–824.

Abdala, C., Luo, P., and Guardia, Y. (**2019**). "Swept-tone stimulus-frequency otoacoustic emissions in human newborns," Trends Hear. **23**, 1–15.

Abdala, C., Luo, P., and Shera, C. A. (**2015**). "Optimizing swept-tone protocols for recording distortion-product otoacoustic emissions in adults and newborns," J. Acoust. Soc. Am. **138**, 3785–3799.

Abdala, C., Luo, P., and Shera, C. A. (**2022**). "Characterizing the relationship between reflection and distortion otoacoustic emissions in normal-hearing adults," J. Assoc. Res. Otolaryngol. **23**, 647–664.

Abdala, C., Ortmann, A. J., and Shera, C. A. (**2018a**). "Reflection- and distortion-source otoacoustic emissions: Evidence for increased irregularity in the human cochlea during aging," J. Assoc. Res. Otolaryngol. **19**, 493–510.

Bader, K., Dalhoff, E., Dierkes, L., Braun, L. H., Gummer, A. W., and Zelle, D. (**2024**). "Reliable long-term serial evaluation of cochlear function using pulsed distortion-product otoacoustic emissions: Analyzing levels and pressure time courses," Ear Hear. **45**, 1326–1338.

Bennett, C. L., and Özdamar, Ö. (**2010**). "Swept-tone transient-evoked otoacoustic emissions," J. Acoust. Soc. Am. **128**, 1833–1844.

31 October 2024 19:47:36

Berezina-Greene, M. A., and Guinan, J. J. (**2015**). "Stimulus frequency otoacoustic emission delays and generating mechanisms in guinea pigs, chinchillas, and simulations," J. Assoc. Res. Otolaryngol. **16**, 679–694.
Bess, F. H. (**1985**). "The minimally hearing-impaired child," Ear Hear. **6**, 43–47.
Bess, F. H., Dodd-Murphy, J., and Parker, R. A. (**1998**). "Children with minimal sensorineural hearing loss: Prevalence, educational performance, and functional status," Ear Hear. **19**, 339–354.
Brown, A. M., and Kemp, D. T. (**1984**). "Suppressibility of the $2f_1$-f_2 stimulated acoustic emission in gerbil and man," Hear. Res. **13**, 29–37.
Charaziak, K. K., and Shera, C. A. (**2017**). "Compensating for ear-canal acoustics when measuring otoacoustic emissions," J. Acoust. Soc. Am. **141**, 515–531.
Choi, Y. S., Lee, S. Y., Parham, K., Neely, S. T., and Kim, D. O. (**2008**). "Stimulus-frequency otoacoustic emission: Measurements in humans and simulations with an active cochlear model," J. Acoust. Soc. Am. **123**, 2651–2669.
Dorn, P. A., Piskorski, P., Gorga, M. P., Neely, S. T., and Keefe, D. H. (**1999**). "Predicting audiometric status from distortion product otoacoustic emissions using multivariate analyses," Ear Hear. **20**, 149–163.
Ellison, J. C., and Keefe, D. H. (**2005**). "Audiometric predictions using SFOAE and middle-ear measurements," Ear Hear. **26**, 487–503.
Glavin, C. C., Dhar, S., and Goodman, S. S. (**2023**). "Measurement of swept level distortion product otoacoustic emission growth functions at multiple frequencies simultaneously," JASA Express Lett. **3**, 064401.
Glavin, C. C., Siegel, J., and Dhar, S. (**2021**). "Distortion product otoacoustic emission (DPOAE) growth in aging ears with clinically normal behavioral thresholds," J. Assoc. Res. Otolaryngol. **22**, 659–680.
Go, N. A., Stamper, G. C., and Johnson, T. A. (**2019**). "Cochlear mechanisms and otoacoustic emission test performance," Ear Hear. **40**, 401–417.
Goodman, S. S., Lee, C., Guinan, J. J., Jr., and Lichtenhan, J. T. (**2020**). "The spatial origins of cochlear amplification assessed by stimulus-frequency otoacoustic emissions," Biophys. J. **118**, 1183–1195.
Gorga, M. P., Dierking, D. M., Johnson, T. A., Beauchaine, K. L., Garner, C. A., and Neely, S. T. (**2005**). "A validation and potential clinical application of multivariate analyses of distortion-product otoacoustic emission data," Ear Hear. **26**, 593–607.
Gorga, M. P., Neely, S. T., Bergman, B., Beauchaine, K. L., Kaminski, J. R., Peters, J., and Jesteadt, W. (**1993a**). "Otoacoustic emissions from normal-hearing and hearing-impaired subjects: Distortion product responses," J. Acoust. Soc. Am. **93**, 2050–2060.
Gorga, M. P., Neely, S. T., Bergman, B. M., Beauchaine, K. L., Kaminski, J. R., Peters, J., Schulte, L., and Jesteadt, W. (**1993b**). "A comparison of transient-evoked and distortion product otoacoustic emissions in normal-hearing and hearing-impaired subjects," J. Acoust. Soc. Am. **94**, 2639–2648.
Gorga, M. P., Neely, S. T., Ohlrich, B., Hoover, B., Redner, J., and Peters, J. (**1997**). "From laboratory to clinic: A large-scale study of distortion product otoacoustic emissions in ears with normal hearing and ears with hearing loss," Ear Hear. **18**, 440–455.
Groon, K. A., Rasetshwane, D. M., Kopun, J. G., Gorga, M. P., and Neely, S. T. (**2015**). "Air-leak effects on ear-canal acoustic absorbance," Ear Hear. **36**, 155–163.
Hudspeth, A., and Corey, D. (**1977**). "Sensitivity, polarity, and conductance change in the response of vertebrate hair cells to controlled mechanical stimuli," Proc. Natl. Acad. Sci. U.S.A. **74**, 2407–2411.
Hussain, D. M., Gorga, M. P., Neely, S. T., Keefe, D. H., and Peters, J. (**1998**). "Transient evoked otoacoustic emissions in patients with normal hearing and in patients with hearing loss," Ear Hear. **19**, 434–449.
Johnson, T. A., Neely, S. T., Kopun, J. G., Dierking, D. M., Tan, H., Converse, C., Kennedy, E., and Gorga, M. P. (**2007**). "Distortion product otoacoustic emissions: Cochlear-source contributions and clinical test performance," J. Acoust. Soc. Am. **122**, 3539–3553.
Kalluri, R., and Shera, C. A. (**2007**). "Comparing stimulus-frequency otoacoustic emissions measured by compression, suppression, and spectral smoothing," J. Acoust. Soc. Am. **122**, 3562–3575.
Kalluri, R., and Shera, C. A. (**2013**). "Measuring stimulus-frequency otoacoustic emissions using swept tones," J. Acoust. Soc. Am. **134**, 356–368.
Kemp, D. T. (**1978**). "Stimulated acoustic emissions from within the human auditory system," J. Acoust. Soc. Am. **64**, 1386–1391.
Kemp, D. T., Bray, P., Alexander, L., and Brown, A. M. (**1986**). "Acoustic emission cochleography—Practical aspects," Scand. Audiol. Suppl. **25**, 71–95.
Kim, D. O., Paparello, J., Jung, M. D., Smurzynski, J., and Sun, X. (**1996**). "Distortion otoacoustic emission test of sensorineural hearing loss: Performance regarding sensitivity, specificity, and receiver operating characteristics," Acta Oto-Laryngol. (Stockholm) **116**, 3–11.
Konrad-Martin, D., Neely, S. T., Keefe, D. H., Dorn, P. A., Cyr, E., and Gorga, M. P. (**2002**). "Sources of DPOAEs revealed by suppression experiments, inverse fast Fourier transforms, and SFOAEs in impaired ears," J. Acoust. Soc. Am. **111**, 1800–1809.
Kummer, P., Janssen, T., and Arnold, W. (**1998**). "The level and growth behavior of the $2f_1$-f_2 distortion product otoacoustic emission and its relationship to auditory sensitivity in normal hearing and cochlear hearing loss," J. Acoust. Soc. Am. **103**, 3431–3444.
Lichtenhan, J. T. (**2012**). "Effects of low-frequency biasing on otoacoustic and neural measures suggest that stimulus-frequency otoacoustic emissions originate near the peak region of the traveling wave," J. Assoc. Res. Otolaryngol. **13**, 17–28.
Long, G. R., Talmadge, C. L., and Lee, J. (**2008**). "Measuring distortion product otoacoustic emissions using continuously sweeping primaries," J. Acoust. Soc. Am. **124**, 1613–1626.
Lonsbury-Martin, B. L., Harris, F. P., Stagner, B. B., Hawkins, M. D., and Martin, G. K. (**1990**). "Distortion product emissions in humans. I. Basic properties in normally hearing subjects," Ann. Otol. Rhinol. Laryngol. **99**, 3–14.
Martin, G. K., Ohlms, L. A., Franklin, D. J., Harris, F. P., and Lonsbury-Martin, B. L. (**1990**). "Distortion product otoacoustic emissions: III. Influence of sensorineural hearing loss," Ann. Otol. Rhinol. Laryngol. **99**, 30–42.
Mauermann, M., and Kollmeier, B. (**2004**). "Distortion product otoacoustic emission (DPOAE) input/output functions and the influence of the second DPOAE Source," J. Acoust. Soc. Am. **116**, 2199–2212.
Maxim, T., Shera, C. A., Charaziak, K. K., and Abdala, C. (**2019**). "Effects of forward- and emitted-pressure calibrations on the variability of otoacoustic emission measurements across repeated probe fits," Ear Hear. **40**, 1345–1358.
Moleti, A., Longo, F., and Sisto, R. (**2012**). "Time-frequency domain filtering of evoked otoacoustic emissions," J. Acoust. Soc. Am. **132**, 2455–2467.
Petley, L., Hunter, L. L., Motlagh Zadeh, L., Stewart, H. J., Sloat, N. T., Perdew, A., Lin, L., and Moore, D. R. (**2021**). "Listening difficulties in children with normal audiograms: Relation to hearing and cognition," Ear Hear. **42**, 1640–1655.
Poling, G. L., Siegel, J. H., Lee, J., and Dhar, S. (**2022**). "The influence of self-reported noise exposure on $2f_1$-f_2 distortion product otoacoustic emission level, fine structure, and components in a normal-hearing population," J. Acoust. Soc. Am. **151**, 2391–2402.
Prieve, B. A., Gorga, M. P., Schmidt, A., Neely, S., Peters, J., Schultes, L., and Jesteadt, W. (**1993**). "Analysis of transient-evoked otoacoustic emissions in normal-hearing and hearing-impaired ears," J. Acoust. Soc. Am. **93**, 3308–3319.
Probst, R., Lonsbury-Martin, B. L., Martin, G. K., and Coats, A. C. (**1987**). "Otoacoustic emissions in ears with hearing loss," Am. J. Otolaryngol. **8**, 73–81.
Reuven, M. L., Neely, S. T., Kopun, J. G., Rasetshwane, D. M., Allen, J. B., Tan, H., and Gorga, M. P. (**2013**). "Effect of calibration method on distortion-product otoacoustic emission measurements at and around 4 kHz," Ear Hear. **34**, 779–788.
Rhode, W. S. (**1971**). "Observations of the vibration of the basilar membrane in squirrel monkeys using the Mössbauer technique," J. Acoust. Soc. Am. **49**, 1218–1231.
Robles, L., and Ruggero, M. A. (**2001**). "Mechanics of the mammalian cochlea," Physiol. Rev. **81**, 1305–1352.
Ruggero, M. A., and Rich, N. C. (**1991**). "Furosemide alters organ of Corti mechanics: Evidence for feedback of outer hair cells upon the basilar membrane," J. Neurosci. **11**, 1057–1067.
Scheperle, R. A., Goodman, S. S., and Neely, S. T. (**2011**). "Further assessment of forward pressure level for *in situ* calibration," J. Acoust. Soc. Am. **130**, 3882–3892.

31 October 2024 19:47:36

Scheperle, R. A., Neely, S. T., Kopun, J. G., and Gorga, M. P. (**2008**). "Influence of *in situ*, sound-level calibration on distortion-product otoacoustic emission variability," J. Acoust. Soc. Am. **124**, 288–300.
Shera, C. A. (**2024**). "Swept along: Measuring otoacoustic emissions using continuously varying stimuli," J. Assoc. Res. Otolaryngol. **25**, 91–102.
Shera, C. A., and Abdala, C. (**2016**). "Frequency shifts in distortion-product otoacoustic emissions evoked by swept tones," J. Acoust. Soc. Am. **140**, 936–944.
Shera, C. A., and Bergevin, C. (**2012**). "Obtaining reliable phase-gradient delays from otoacoustic emission data," J. Acoust. Soc. Am. **132**, 927–943.
Shera, C. A., and Guinan, J. J., Jr. (**1999**). "Evoked otoacoustic emissions arise by two fundamentally different mechanisms: A taxonomy for mammalian OAEs," J. Acoust. Soc. Am **105**, 782–798.
Smurzynski, J., and Kim, D. O. (**1992**). "Distortion-product and click-evoked otoacoustic emissions of normally-hearing adults," Hear. Res. **58**, 227–240.
Souza, N. N., Dhar, S., Neely, S. T., and Siegel, J. H. (**2014**). "Comparison of nine methods to estimate ear-canal stimulus levels," J. Acoust. Soc. Am. **136**, 1768–1787.
Stiepan, S., Goodman, S. S., and Dhar, S. (**2022**). "Optimizing distortion product otoacoustic emission recordings in normal-hearing ears by adopting cochlear place-specific stimuli," J. Acoust. Soc. Am. **152**, 776–788.
Stiepan, S., Shera, C. A., and Abdala, C. (**2023**). "Characterizing a joint reflection-distortion OAE profile in humans with endolymphatic hydrops," Ear Hear. **44**, 1437–1450.
Stover, L., Gorga, M. P., Neels, S. T., and Montoya, D. (**1996**). "Towards optimizing the clinical utility of distortion product otoacoustic emission measurements," J. Acoust. Soc. Am. **100**, 956–967.
Swets, J. A. (**1988**). "Measuring the accuracy of diagnostic systems," Science **240**, 1285–1293.
Swets, J. A., and Pickett, R. M. (**1982**). *Evaluation of Diagnostic Systems: Methods from Signal Detection Theory* (Academic, New York).
Whitehead, M. L., Stagner, B. B., Martin, G. K., and Lonsbury-Martin, B. L. (**1996**). "Visualization of the onset of distortion-product otoacoustic emissions and measurement of their latency," J. Acoust. Soc. Am. **100**, 1663–1679.
Zelle, D., Dalhoff, E., and Gummer, A. W. (**2017a**). "Objective audiometry with DPOAEs: New findings for generation mechanisms and clinical applications," HNO **65**, 122–129.
Zelle, D., Lorenz, L., Thiericke, J. P., Gummer, A. W., and Dalhoff, E. (**2017b**). "Input-output functions of the nonlinear-distortion component of distortion-product otoacoustic emissions in normal and hearing-impaired human ears," J. Acoust. Soc. Am. **141**, 3203–3219.
Zelle, D., Thiericke, J. P., Dalhoff, E., and Gummer, A. W. (**2015**). "Level dependence of the nonlinear-distortion component of distortion-product otoacoustic emissions in humans," J. Acoust. Soc. Am **138**(6), 3475–3490.
Zweig, G., and Shera, C. A. (**1995**). "The origin of periodicity in the spectrum of evoked otoacoustic emissions," J. Acoust. Soc. Am. **98**, 2018–2047.

31 October 2024 19:47:36